

AD-A044 617

GEORGIA INST OF TECH ATLANTA SCHOOL OF CHEMICAL ENGI--ETC F/G 11/6
THE CYCLIC STRESS-STRAIN RESPONSE OF TITANIUM-VANADIUM ALLOYS.(U)
AUG 77 S B CHAKRABORTTY, T K MUKHOPADHYAY N00014-75-C-0349

UNCLASSIFIED

GIT-TR-77-1

NL

| OF |
ADA
044617



AD A 044617

OFFICE OF NAVAL RESEARCH

12
B.S.

Contract N00014-75-C-0349, NR 031-750

TECHNICAL REPORT 77-1

**THE CYCLIC STRESS-STRAIN RESPONSE
OF TITANIUM-VANADIUM ALLOYS**

By

**S. B. Chakraborty, T. K. Mukhopadhyay,
and E. A. Starke, Jr.**

August 30, 1977

1977

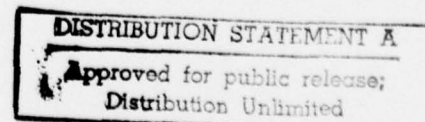


**Metallurgy Program, School of Chemical Engineering
Georgia Institute of Technology
Atlanta, Georgia 30332**



**Reproduction in whole or in part is permitted for any
purpose of the United States Government**

Distribution of this document is unlimited



AD No. _____
DDC FILE COPY.

15 OFFICE OF NAVAL RESEARCH
Contract N00014-75-C-0349, NR 031-750

7 TECHNICAL REPORT, 77-1

6 THE CYCLIC STRESS-STRAIN RESPONSE
OF TITANIUM-VANADIUM ALLOYS,

by

10 S. B./Chakraborty, T. K./Mukhopadhyay and E. A./Starke, Jr.
School of Chemical Engineering and Metallurgy
Georgia Institute of Technology
Atlanta, Georgia 30332

14 GITL-TR-77-1

11 30 August 30, 1977

12 11/1/77

Reproduction in whole or in part is permitted for any purpose of
the United States Government.

Distribution of this document is unlimited.

409996

DISTRIBUTION STATEMENT A
Approved for public release; Distribution Unlimited

DDC
RECEIVED
SEP 28 1977
B
LB

THE CYCLIC STRESS-STRAIN RESPONSE
OF TITANIUM-VANADIUM ALLOYS

S. B. Chakraborty, T. K. Mukhopadhyay
and E. A. Starke, Jr.

School of Chemical Engineering and Metallurgy
Georgia Institute of Technology
Atlanta, Georgia 30332

ABSTRACT

The cyclic stress-strain response of four Ti-V alloys (24, 28, 32 and 36wt.% V), which have deformation modes ranging from coarse twinning to wavy and planar slip, has been measured and correlated with deformation mode and microstructure. When coarse twinning is the primary deformation mode an anomalous Bauschinger effect, associated with untwinning during load reversal, is observed. A saturation flow stress is not obtained for the wavy slip alloy due to the intervention of microtwinning which inhibits cross slip and cell formation. Cyclic hardening of all alloys appears to be related, in some degree, to deformation twinning. Cyclic softening occurs for the planar slip alloys in the absence of microtwinning due to increasing mobile dislocation density.

ACCESS TO	
NTIS	<input checked="" type="checkbox"/>
DOC	<input type="checkbox"/>
UNCLASSIFIED	<input type="checkbox"/>
JUSTIFICATION	<input type="checkbox"/>
BY	
DISTRIBUTION/AVAILABILITY CODES	
Dist.	ALL and/or SPECIAL
A	

INTRODUCTION

Laird^(1,2) has recently reviewed the cyclic deformation of metals and alloys and has described the rapid hardening or softening which occurs in the early stages of fatigue life. It is clear from his reviews that the majority of work has been on fcc materials having either planar or wavy slip character, and very few studies have been concerned with the effect of alloying and deformation mode on the cyclic stress strain response of bcc metals. In addition, to the author's knowledge, there has been no previous study of ductile bcc alloys whose primary deformation mode is twinning. This paper is concerned with the cyclic stress strain response of a series of Ti-V alloys having deformation modes which vary from coarse twinning to wavy and planar slip.

Our previous studies⁽³⁻⁶⁾ have shown that the deformation mode and ductility of titanium alloys containing from 20 to 40 weight percent vanadium can be controlled to a large extent by solute content and volume fraction of omega. Slip has been observed to change in character from fine wavy slip to coarse planar slip as the solute content is increased from 28% V to 40% V⁽³⁾. Both {110} and {112} slip occurs in the 28% V alloy, although {110} slip dominates, whereas planar {112} slip dominates in the 40% V alloy. In addition, {112} <111> twinning has been identified as an important deformation mode in the Ti-V system and can be controlled by proper solute content and thermal treatment. A change in deformation mode from slip to coarse twinning, with no loss in ductility, occurs in the low solute (20, 24, 28% V) alloys when the volume fraction of omega exceeds ~ 0.1. Volume fractions larger than 0.6 result in partial or complete

embrittlement with an accompanied change in deformation mode from coarse twinning to slip. The onset of α precipitation in alloys containing less than 0.6 omega also induces a transition from coarse twinning to a mixture of fine twins and slip but without excessive loss in ductility. $\{112\} \langle 111 \rangle$ twins have been observed in electron micrographs of the 40% V alloy, but are too fine to be detected optically. X-ray line broadening measurements⁽³⁾ have shown that a minimum in the twin fault probability exists for this system at 36% V.

The coarse twinning behavior in the low solute alloy is unusual since it is associated with the presence of omega, whose structure is incompatible with the $a/6 \langle 111 \rangle$ twinning shears of the bcc matrix. Dark-field and electron diffraction analysis showed that the $\{\bar{1}\bar{1}2\} \langle 111 \rangle$ coarse twins contain omega precipitates suggesting a stress assisted $\omega \rightleftharpoons \beta$ transformation during deformation twinning.⁽⁶⁾ If the twinning mechanism is associated with a reversible omega transformation, and there is extensive evidence supporting this view^(6,7), untwinning may occur under reversed or cyclic loading similar to that of Fe-Be⁽⁸⁾ or the shape-memory alloy Au-Cd⁽⁹⁾. Such pseudoelastic effects can greatly effect the cyclic stress strain response and fatigue life of alloys⁽¹⁰⁻¹²⁾.

The Ti-V system offered the possibility of studying the CSSR of bcc alloys having wavy and planar slip character, with the added bonus that the effects of both coarse and fine deformation twinning could be examined.

EXPERIMENTAL

Four Ti-V alloys, containing 24, 28, 32, and 36 weight percent vanadium were prepared by argon arc melting 99.95 percent purity

starting materials. The 50 gram ingots were vacuum encapsulated in quartz and homogenized for 100 hours at 950°C. They were then cold rolled in a random fashion to obtain a uniform thickness of 5 mm, recrystallized under vacuum for two hours at 850°C (above the β transus) and quenched in water. The recrystallized samples had a uniform grain size of ~ 0.2 mm and a random texture. In addition, a 24% V alloy was prepared by Titanium Metals Corporation, Henderson, Nevada, where 14 cm diameter ingots were hot-forged and cross-rolled to produce plates 15 cm x 15 cm x 0.8 cm, having a random texture and an equiaxed grain size of ~ 0.10 mm. The chemical analysis of this alloy is given in Table 1. Samples from the as-received plates were solutionized at 850°C and quenched in water. Property differences between laboratory and commercially prepared materials were within experimental error and measurements from the different lots are not distinguished in this paper.

As described in the Introduction, significant differences in deformation character exists for the selected alloys in the as-solutionized and quenched conditions. The microstructure and deformation behavior were characterized by x-ray diffraction, optical, scanning, and electron microscopy using procedures described previously⁽³⁻⁵⁾. Monotonic and cyclic property measurements were made on all alloys in the as-quenched condition, and after various heat treatments which were chosen to slightly alter the microstructure and deformation characteristics. The heat treatment, resulting microstructure, deformation characteristics, and tensile properties are listed in Table 2. Tensile samples were machined according to ASTM E-8-66 for sub-size specimens, and

tests were made at a strain rate of 10^{-3} /sec on an Instron testing machine equipped with a 1-in clip-on extensometer.

Low cycle fatigue samples were smooth and cylindrical, with a gage section approximately 6 mm long by 3.5 mm diameter, and were polished through a 1 μ alumina and chromium oxide solution to remove all circumferential scratches. Most cyclic-stress-strain measurements were made on an electrohydraulic, closed-loop MTS testing machine under constant total strain control, with saw-tooth wave form, and at a strain rate of 10^{-3} /sec. However, the erratic response of the closed-loop system under strain control during deformation twinning of the 24% V alloy necessitated the use of stroke control for its CSS measurements. Strain was monitored by a 4 mm clip-on extensometer and the stroke was changed throughout the test so that the plastic strain range remained essentially constant.

RESULTS AND DISCUSSION

Coarse Twinning Conditions

The combination of vanadium content and quenching speed was not sufficient to suppress the omega formation in the 24% V alloy, and the primary deformation mode of the as-quenched condition was coarse twinning. The aged samples contained some alpha and showed a greater propensity for slip and an accompanying reduction in ductility, Table 2. The cyclic-stress-strain loops showed anomalies at the low strain amplitudes similar to those observed by Bolling and Richmond⁽⁸⁾ for spontaneous untwinning in single crystals of Fe-25 at. % Be, although the magnitude of the effect was somewhat less in our polycrystalline samples. The Bauschinger effect, Figure 1, which is indicative of

the type III kinematic hardening described by Asaro^(13,14), was measured by the method of Stoltz and Pelloux,⁽¹⁵⁾ Figure 2. The Bauschinger back stress, $\Delta\sigma_b$, is indicative of the ease of recovery of the forward strain and the reversed Bauschinger strain, β , shows the extent of the recovery. Since a change in $\Delta\sigma_b$ indicates a similar change in β and since less error is involved in the measurement of $\Delta\sigma_b$, most conclusions in this paper are drawn from the values of $\Delta\sigma_b$. The Bauschinger back stress for the first cycle, $\Delta\sigma_b^1$, decreased with increasing strain amplitude, Figure 3a. The Bauschinger back stress also decreased with cycling at constant strain amplitude, Figure 3b. A greater strain dependency was observed for the aged samples which deformed by both twinning and slip. The reversed Bauschinger strain, β^{+1} , was almost completely recoverable for forward strain amplitudes up to 2% for both conditions tested, Figure 3c. The shape of the hysteresis loop was not symmetric, the compression side being narrower than the tension side, i.e., $B_- < B_+$. This is associated with a higher strength of the alloy in compression and was observed for both stroke and total strain control. The effect was larger for smaller strain amplitudes and diminished during the later part of life, Figure 4.

The anomalous Bauschinger effect described above is very similar to the pseudoelasticity associated with reversible stress-induced martensitic transformations in shape-memory alloys (for review, see Delaey et al.⁽¹⁶⁾). This is not surprising when one considers the similarity between deformation twinning and martensite reactions^(17,18), and the fact that twinning in these low-solute alloys is associated with a stress-induced reversion of omega⁽⁷⁾. How and why this occurs is

not clear; however, it is evident that some type of energy absorption is associated with twinning (in addition to elastic accommodation energy). For small forward strains, small undamaged twins are formed and the twin energy is not dissipated. Consequently the twins should untwin to matrix when the applied stress is removed, Figure 1. For large strain amplitudes, the twins are damaged by interactions from other twins and dislocations, and some of the elastic accommodation energy is dissipated. Therefore, only part of the total energy associated with a twin is recoverable upon unloading and the Bauschinger back stress, which is a measure of the ease of stored energy recovery, decreases with increasing strain amplitude. The effect is magnified as the propensity for slip increases, as observed for the aged alloy.

It is known that deformation twin growth generates lattice defects in the vicinity of the twin interface, and as a consequence untwinning does not occur uniformly along the interface resulting in fragmented and damaged twins. This is quite evident when comparing the optical micrograph of twins formed under monotonic deformation, Figure 5a, with the optical micrograph of damaged twins formed under cyclic deformation, Figure 5b. A transmission electron micrograph of the damaged twins is shown in Figure 5c. In addition, untwinning leaves dislocation damage and accommodation kinking.⁽¹⁹⁾ Consequently, the absorbed energy due to twinning is never completely recoverable during reversed loading, even for low strain amplitudes, and as cycling continues the Bauschinger back stress decreases as the accumulated plastic strain increases, Figure 3b.

The results of the low cycle fatigue tests are presented for the as-quenched, and aged 24% V alloy in Figures 6 and 7 respectively, as: (a) average cyclic stress amplitude versus accumulated plastic strain, (b) log of the plastic strain amplitude versus log of the number of reversals for crack initiation and (c) logarithmic monotonic and cyclic stress strain curves. The termination points of the curves in Figures 6a and 7a correspond to the first visual observation of cracks. The fatigue ductility coefficients, ϵ_f' , the Coffin-Manson slopes, $-c$, and the monotonic and cyclic work hardening exponents n and n' , are given on the Figures. The differences in these data for the two conditions was minimal, as would be expected since only small differences in deformation behavior were observed. The fatigue hardening observed for this alloy was the largest for any of the alloys tested, and saturation was never reached for any strain amplitude. Cyclic hardening began on the first cycle for the larger strain amplitudes; however, for the smaller strain amplitudes, the stress amplitude remained essentially constant for as many as 30 cycles before hardening commenced. The large degree of cyclic hardening is associated with twin interfaces acting as barriers to continued deformation and with lattice defects generated by the twinning mechanism. The lack of initial hardening observed during the low strain amplitude tests is associated with the reversibility of the deformation process, i.e., untwinning. However, as described previously, this reversibility disappears with cycling, at which time hardening begins. The twins formed at low strain amplitudes were smaller than those formed at high strain amplitudes, creating more interfaces and resulting in a relatively larger total hardening

effect for low strain amplitude cycling than for high strain amplitude cycling. This is reflected in the small cyclic hardening exponent, n' , compared with the monotonic hardening exponent, n .

In order to study the effect of the large twins produced at high strain amplitudes on the cyclic hardening behavior at low strain amplitudes, a few samples were cycled as follows: one complete cycle at a strain amplitude of $\Delta\epsilon_p/2 = 2.7\%$, followed by three cycles at $\Delta\epsilon_p/2 = 1.3\%$, and then cycled to failure at $\Delta\epsilon_p/2 = 0.1\%$. Figure 8 shows the results of this test, curve 2, along with a sample cycled to failure at a constant strain amplitude of $\Delta\epsilon_p/2 = 0.1\%$, curve 1. Curve 2 always falls below curve 1 for the same $\Delta\epsilon_p/2$. The high strain amplitude deformation results in large damaged twins within the grains. The presence of these twins reduces the propensity for further deformation twinning, and thus inhibits the formation of the numerous small (and relatively undamaged) twin interfaces responsible for the rapid hardening observed in the constant low strain amplitude test; AB in Figure 8. Consequently, the hardening is far less rapid for the variable strain amplitude test; FG in Figure 8. The rapid hardening observed along EF is due to the reduction in reversibility of the small twins caused by the presence of large damaged twin interfaces. A comparison of the twins produced in the constant amplitude test with those produced in the variable amplitude test is shown in Figure 9 (a and b). The most striking effect of the variable loading was its influence on crack propagation. The difference between N_f and N_i was approximately 1100 cycles for the variable loaded samples and approximately 15 cycles for the constant amplitude samples. Further crack propagation studies are now underway.

The Coffin-Manson-type plots for the two conditions tested for the 24% V alloy have unusually large slopes $|c|$ and had a distinct break at low strain amplitudes similar to those observed for aluminum alloys.^(20,21) It has been noted previously⁽²¹⁾ that the deviation from the semi-empirical prediction of the Coffin-Manson relationship is related to the fatigue deformation processes prior to crack initiation; as must be the case here since the cycles to initiation, and not failure, are used for the abscissa. The resistance to fatigue crack initiation depends upon the homogeneity and reversibility of deformation. When deformation is reversible the damage is not accumulated to a great extent with cycling, and when it is homogeneous the accumulation is not localized. Since the deformation mode, i.e., twinning, is not reversible for large accumulated strains, and is accompanied by slip dislocations and formation of other lattice defects, a stable microstructure is never formed, resulting in early crack initiation and therefore a large $|c|$. The worst situation occurs at low strain amplitudes, because here the deformation is not only irreversible but also inhomogeneous.

There have been numerous observations^(19,22) that plastic deformation is enhanced parallel to a twin boundary and that this localized slip leads to cracking at the twin matrix interface. The fact that the slip and twinning planes are the same in the Ti-V system suggests that this mechanism may be responsible for early crack initiation. Concentrated slip was observed near twin bands prior to crack initiation, Figure 10a, and cracks were later observed along the twin bands, Figure 10b.

Wavy Slip Condition

The as-quenched 28% V alloy was all beta phase (no omega detected by x-ray diffraction) and optical examination of deformed tensile samples revealed fine wavy slip and no deformation twins. The anomalous Bauschinger effect, observed for the 24% V alloy, was absent during cyclic deformation and measurements of the normal type I^(13,14) Bauschinger strain were not made. The results of the low cycle fatigue test are presented in Figure 11. Unlike most materials that deform by wavy slip,^(1,2,23,24) a saturation flow stress was never reached and cyclic hardening persisted until crack-initiation, Figure 11a. The magnitude of the hardening and the Coffin-Manson slope, $|c|$, were somewhat smaller than those observed for the 24% V alloy.

Optical examination of surface slip bands and polished cross sections of samples cycled to failure, Figure 12, confirmed that the primary deformation mode was wavy slip; at least on a macroscopic scale. No coarse deformation twins were observed. Although most similar studies have been on fcc metals and alloys, low cycle fatigue studies of iron^(24,25) have shown that a saturation flow stress is obtained during cyclic deformation of that wavy-slip bcc metal. The related microstructure had well defined cells⁽²⁵⁾, analogous to those found in fcc metals.⁽²⁶⁾ Transmission electron microscopy studies of LCF samples of our as-quenched 28% V alloy revealed mostly wide deformation bands, Figure 13a, although microtwins were frequently observed, Figure 13b. Consequently, one must conclude that the wavy slip character observed optically is not due to the cross slip of screw dislocation which is normally associated with the

spreading of glide from two to three dimensions, but is most likely associated with the multiple slip systems previously observed for this alloy.⁽⁴⁾ The lack of saturation and cell formation may be due to the intervention of a different deformation process, i.e., twinning, which inhibits dynamic recovery by cross slip and leads to early crack initiation in these strain controlled tests. In addition, connected cross-slip may be hindered by stress-induced omega precipitation similar to that detected in our early work on cold-rolled Ti-28%V single crystals.⁽³⁾ The absence of a saturation stress, extensive hardening and lack of cell formation, similar to that observed here, was found in an Fe-1.5% Cu alloy containing noncoherent precipitate particles.⁽²⁷⁾ The authors concluded that the small precipitates were the cause of the continuous cyclic hardening and lack of cell formation.

In order to study the effect of a very small volume fraction of omega on the cyclic stress strain response of the Ti-28% V alloy, samples were aged for 360 minutes at 300°C. Previous hardness studies⁽⁵⁾ had indicated that a small amount (less than can be routinely detected by x-ray diffraction) of isothermal omega is formed for this time, temperature, and vanadium concentration. The results of the low-cycle fatigue tests are shown in Figure 14, and should be compared with the as-quenched data of Figure 11. The cyclic hardening behavior and Coffin-Manson slopes, $|c|$, are very similar for the two conditions, as are the optically observed slip markings, Figure 15a. Transmission electron micrographs, Figure 15b, showed deformation structures similar to those of the fatigued as-quenched samples. However, omega precipitates were far more numerous than observed in deformed as-quenched samples.

The larger volume fraction of precipitates can certainly account for the higher strength of the aged alloy; however, the similarity in hardening behavior appears to be more related to the deformation mode and microtwin formation. This conclusion is drawn from the fact that although the amount of omega precipitates in the aged samples was considerably higher than in the deformed as-quenched samples, the magnitude of the cyclic hardening was essentially the same.

Planar Slip Conditions

The as-quenched 32% V and 36% V alloys contained all beta phase and optical examination of deformed tensile samples revealed coarse planar slip and no deformation twins. Previous studies^(4,28,29) have shown that planar {112} slip dominates in these bcc Ti-V alloys. No anomalous Bauschinger effect was observed and Bauschinger strain measurements were not made. The results of the low cycle fatigue tests are presented in Figures 16 and 17. The Coffin-Manson slopes, $|c|$, were smaller than found for the other two alloys, and approximately equal to that found for most materials, i.e., ~ 0.5 . The cyclic hardening/softening behavior was somewhat anomalous, in that cyclic softening was observed for low strain amplitude tests while cyclic hardening was found for high strain amplitude tests, Figures 16a, c and 17a, c.

Optical examination of polished cross sections of fatigued samples showed planar slip for all conditions, Figure 18, although there were some minor differences in homogeneity of slip band distribution. Transmission electron microscopy studies did, however, reveal differences which could at least qualitatively account for the hardening/

softening observed for the high/low strain amplitude tests. Foils taken from samples of both alloys, which were fatigued to failure at low strain amplitudes where softening occurred, revealed inhomogeneous deformation as ill defined dislocation bands separated by dislocation debris, Figure 19a. No microtwins were observed in any of these failures. In contrast, relatively homogeneous deformation, represented by evenly distributed dislocation debris and microtwins, Figure 19b, was observed in foils from as-quenched samples showing moderate cyclic hardening.

Cyclic softening, similar to that observed here, was found by Koss et al.^(29,30) for a Ti-40 at.% V alloy cycled at a plastic strain amplitude of 0.5%. They concluded that the softening was not due to a metallurgical instability, but a result of dislocation dynamics wherein the mobile dislocation density increases in the presence of a high drag stress and low work hardening rate. We agree with their interpretation of the softening behavior. Koss did not observe cyclic hardening; however, he did not conduct tests at strain amplitudes as large as those that produced hardening in this study. Our earlier suggestion that the hardening behavior is associated with deformation twinning in this alloy system is supported by the microstructural study of the 32% V and 36% V alloys. The as-quenched alloys contained no precipitates, and in all cases where hardening occurred, microtwins were found; whereas microtwins were never observed for the conditions where softening occurred. Koss⁽³¹⁾ has also never observed twinning in cyclic softened samples.

In order to collect more information on this hypothesis, low cycle fatigue tests were conducted on Ti-32% V and Ti-35% V samples aged to produce precipitates which enhance twinning, i.e., omega, and

homogenize slip, i.e., α . The results of these tests are presented in Figures 20, 21, and 22. No major differences in LCF behavior was observed in these aged alloys when compared with the results of their as-quenched counterparts. The Coffin-Manson slopes were essentially the same, cyclic softening was observed at low strain amplitudes and cyclic hardening at high strain amplitudes. Microtwins were infrequently observed in the aged cyclic-softened samples, and were certainly far fewer than observed in as-quenched cyclic hardened samples.

CONCLUSIONS

1. Alloys which deform by coarse twinning exhibit an anomalous Bauschinger effect due to untwinning during reversed loading. Large cyclic hardening was due to twin interfaces acting as barriers to continued cyclic deformation and with lattice defects generated by the twinning mechanism. Crack initiation is associated with concentrated slip near twin bands.
2. Alloys which deformed by wavy slip exhibited cyclic hardening and no saturation prior to crack initiation. The wavy slip character was due to multiple slip and not connected cross slip of screw dislocations. The lack of saturation and cell formation was associated with the intervention of deformation twinning which prevented dynamic recovery by cross slip.
3. Alloys which deformed by planar slip showed cyclic softening at low strain amplitudes and cyclic hardening at high strain amplitudes. The softening behavior is associated with dislocation dynamics and the hardening behavior with deformation twinning.

4. The hardening behavior of all the Ti-V alloys examined is due, at least in part, to deformation twinning inhibiting dynamic recovery.
5. Although the large Coffin-Manson slopes, $|c|$, of the alloys that showed extensive twinning indicate inferior fatigue performance in these strain controlled tests, their cyclic hardening behavior suggests that they may be superior in stress controlled applications.

REFERENCES

1. Campbell Laird in Plastic Deformation of Materials, R. J. Arsenault, ed., pp. 101-102, Academic Press, San Francisco, 1975.
2. Campbell Laird in Work Hardening in Tension and Fatigue, Anthony W. Thompson, ed., pp. 150-176, AIME, New York, 1977.
3. Fu-Wen Ling, H. J. Rack, and E. A. Starke, Jr., Met. Trans., 4, (1973) 1671.
4. Fu-Wen Ling, E. A. Starke, Jr., and B. G. LeFevre, Met. Trans., 5, (1974) 179.
5. H. G. Paris, B. G. LeFevre, and E. A. Starke, Jr., Met. Trans. 7A, (1976) 273.
6. H. G. Paris, B. G. LeFevre, and E. A. Starke, Jr., "The Deformation Twinning Behavior of $\beta + \omega$ Microstructure in Ti-V Alloys," Technical Report 76-1 Office of Naval Research Contract N00014-75-C-0349, NR 031-750, June 15, 1976.
7. H. G. Paris, Ph.D. Thesis, Georgia Institute of Technology, Atlanta, Georgia, August, 1975.
8. G. F. Bolling and R. H. Richman, Acta Met., 13, (1965) 709, 723, 745.
9. D. S. Lieberman, M. A. Schmerling and R. W. Kary, in Shape Memory Effects in Alloys, J. Perkins, ed., pp 203-244, Plenum Press, New York, 1975.
10. W. A. Rochinger, Brit. J. Appl. Phys., 9, (1958) 250; J. Aust. Inst. Metals, 5, (1960) 114.
11. W. J. Buehler and F. W. Wang, Ocean Eng., 1, (1968) 105.
12. N.Y.C. Yang, C. Laird and D. P. Pope, Met. Trans. A, 8A, (1977) 955.
13. R. J. Asaro, Acta Met., 23, (1975) 1255.
14. R. J. Asaro, in Work Hardening in Tension and Fatigue, Anthony W. Thompson, ed., pp 206-223, AIME, New York, 1977.
15. R. E. Stoltz and R. M. Pelloux, Met. Trans A., 7A, (1976) 1295.
16. L. Delsey, R. V. Krishnan, H. Tas, and H. Warlimont, J. Mat. Sci., 9, (1974), p 1521, 1536, and 1545.

17. Robert E. Reed-Hill, Physical Metallurgy Principles, D. Van Nostrand Co., Inc., New Jersey, 1964, p 399.
18. D. V. Wield and E. Gillam, Acta Met., 25, (1977) p 725.
19. P. G. Partridge, Phil. Mag., 12, (1965) p 1043.
20. T. H. Sanders, Jr. and E. A. Starke, Jr., Met. Trans. A, 7A, (1976) p 1407.
21. R. E. Sanders, Jr. and E. A. Starke, Jr., Mat. Sci. & Eng., 28, (1977) p 53.
22. I. A. Gendin and Ya. D. Starodubov, Soviet Physics - Solid State, 2, (1960) p 968.
23. C. E. Feltner and C. Laird, Acta Met., 15, (1967) p 1621.
24. C. E. Feltner and C. Laird, Trans. TMS-AIME, 245, (1969) p 1372.
25. H. Abdel-Raouf and A. Plumtree, Met. Trans., 2, (1971) p 1251.
26. D. Kuhlmann-Wilsdorf and C. Laird, Mat. Sci. & Eng., 27 (1977) p 137.
27. J. T. McGrath and W. J. Bratina, Phil. Mag., 21, (1970) p 1087.
28. N. E. Paton and J. C. Williams in Second Inter. Conf. on the Strength of Metals and Alloys, Asilomar, Pacific Grove, California, (1970) Vol. 1, Paper 1.8 p 108.
29. Donald A. Koss and Craig C. Wocik, Met. Trans A, 7A, (1976) p 1243.
30. G. Theodorski and D. A. Koss, to be published in Third Int. Conf. on Ti (Moscow, May, 1976).
31. Donald A. Koss, Michigan Technological University, Houghton, Michigan, private communication, 1977.

TABLE 1
Compositions of the Titanium-Vanadium Alloy

Alloy	V	Fe	O	N	Ti
Ti-24	24.1	0.04	0.06	0.007	Balance

TABLE 2

Alloy	Heat Treatment	Microstructure	Deformation Mode	Yield Strength $\sigma_{0.2}$ (MPa)	$\epsilon_f (\ln \frac{a_0}{a_f})$
1a Ti-24V	As-Quenched	β + athermal ω	Primarily Coarse Twins	520	0.82
1b Ti-24V	90 min @ 515°C	β + α + athermal ω	Coarse Twins + Slip	565	0.51
2a Ti-28V	As-Quenched	β + ω	Fine Wavy Slip + Microtwins	618	0.63
2b Ti-28V	360 min @ 300°C	β + ω	Primarily Wavy Slip + Twins	720	0.50
3a Ti-32V	As-Quenched	β + ω	Planar Slip	782	0.47
3b Ti-32V	4700 min @ 350°C	β + ω	Fine Slip	956	0.46
4a Ti-36V	As-Quenched	β + ω + α	Coarse Planar Slip	664	0.86
4b Ti-36V	100 min @ 400°C	β + ω + α	Fine Slip	772	0.72
4c Ti-36V	10,000 min @ 400°C	β + α	Fine Slip	880	0.11

FIGURE CAPTIONS

1. Cyclic stress strain response during the first cycle for Ti-24%V at various strain amplitudes showing an anomalous Bauschinger effect.
2. Graphical construction for measuring the Bauschinger effect. After Stoltz and Pelloux.⁽¹⁵⁾
3. Bauschinger Stress and strain data for Ti-24%V alloy.
4. Graphical representation of asymmetry of hysteresis loop with fatigue life for Ti-24%V alloy.
5. Deformation structure of as-quenched Ti-24%V alloy. (a) Optical micrograph after monotonic deformation. (b) Optical micrograph after cyclic deformation (c) TEM after cyclic deformation.
6. Low cycle fatigue behavior of Ti-24%V, as-quenched. (a) stress amplitude vs. accumulative plastic strain, (b) Coffin-Manson plot, (c) cyclic and monotonic stress-strain curves
7. Low cycle fatigue behavior of Ti-24%V, aged 90 minutes at 515°C.
8. Cyclic hardening curves for Ti-24%V alloy using a constant strain amplitude, curve 1; and a variable strain amplitude, curve 2.
9. Deformation twins produced under cyclic straining of Ti-24%V. (a) constant strain amplitude, (b) variable strain amplitude.
10. Scanning electron micrograph of the surface of Ti-24%V fatigue samples. (a) concentrated slip near twin bands, (b) crack along twin bands.
11. Low cycle fatigue behavior of Ti-28%V, as quenched.
12. Optical micrograph of polished and etched cross section of Ti-28%V fatigue sample.
13. Transmission electron micrographs of Ti-28%V fatigue sample. (a) deformation bands, (b) microtwins.
14. Low cycle fatigue behavior of Ti-28%V aged 360 minutes at 300°C.
15. Deformation structure of fatigue samples of aged 360 minutes at 300°C. (a) Optical micrograph (b) transmission electron micrograph.
16. Low cycle fatigue behavior of Ti-32%V, as quenched.

17. Low cycle fatigue behavior of Ti-36%V, as quenched.
18. Optical micrograph showing typical slip markings observed in polished and etched cross sections of as quenched fatigue samples of both 32% and 36% alloys.
19. Typical deformation structure of as quenched fatigued 32% and 36% V alloys. (a) low strain amplitude where cyclic softening occurred. (b) high strain amplitude, where moderate hardening occurred.
20. Low cycle fatigue behavior of Ti-32%V aged 4,700 minutes at 350°C.
21. Low cycle fatigue behavior of Ti-36%V aged 100 minutes at 400°C.
22. Low cycle fatigue behavior of Ti-36%V aged 10,000 minutes at 400°C.

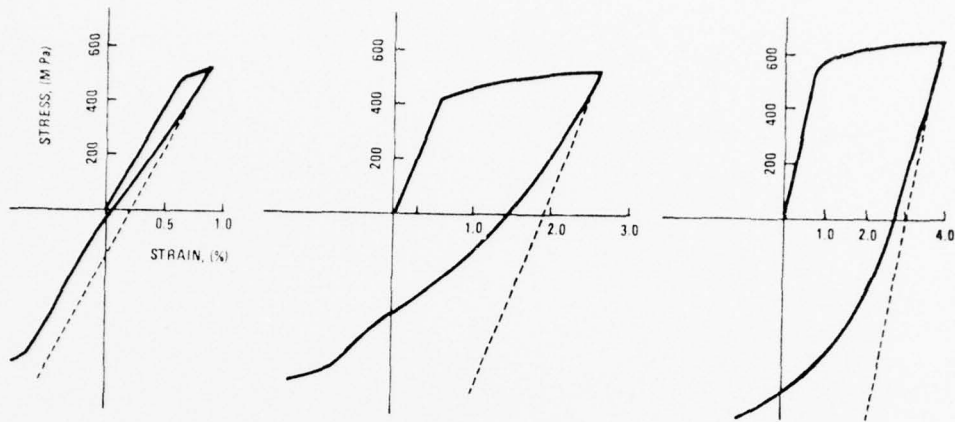


Figure 1. Cyclic stress strain response during the first cycle for Ti-24%V at various strain amplitudes showing an anomalous Bauschinger effect.

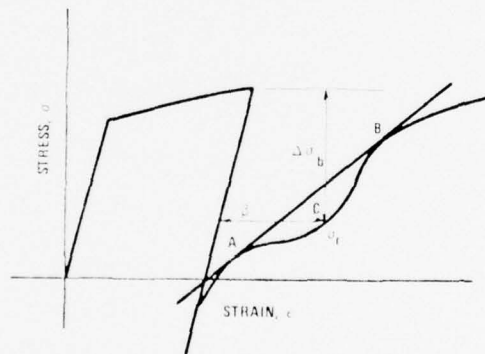


Figure 2. Graphical construction for measuring the Bauschinger effect. After Stoltz and Pelloux. (15).

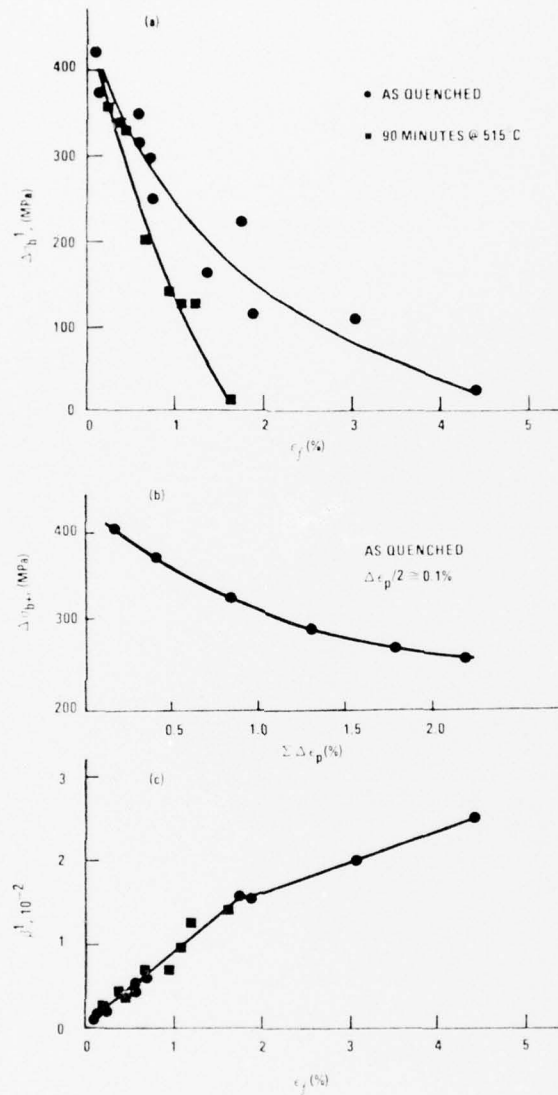


Figure 3. Bauschinger stress and strain data for Ti-24%V alloy.

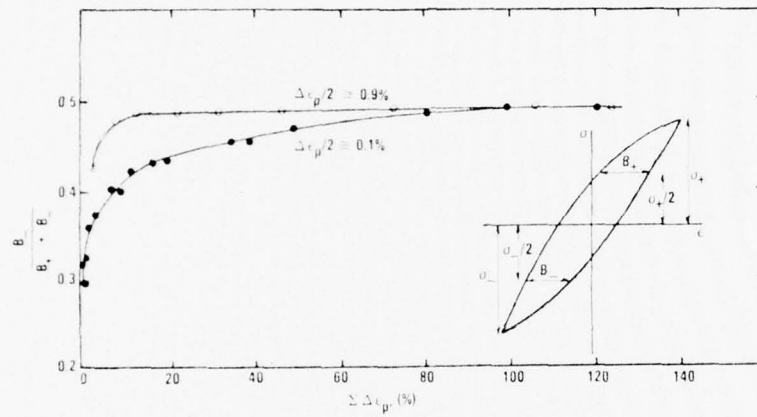
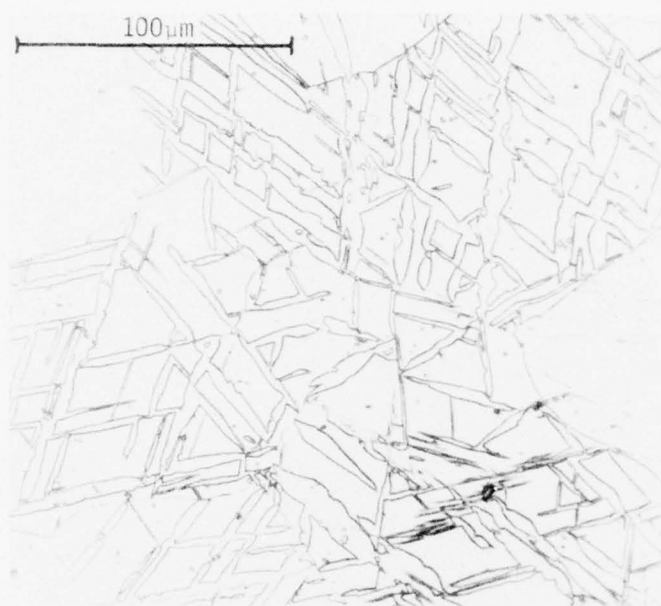
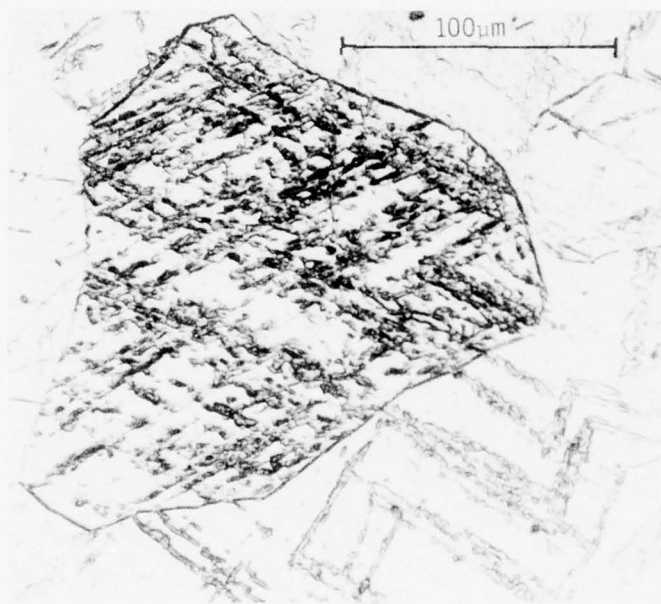


Figure 4. Graphical representation of asymmetry of hysteresis loop with fatigue life for Ti-24%V alloy.



5a



5b



5c

Figure 5. Deformation structure of as-quenched Ti-24%V alloy. (a) Optical micrograph after monotonic deformation. (b) Optical micrograph after cyclic deformation (c) TEM after cyclic deformation.

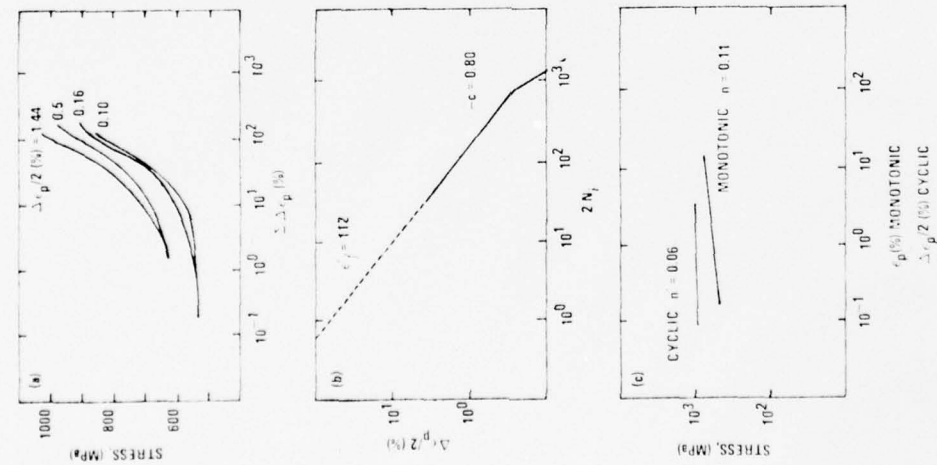


Figure 6. Low cycle fatigue behavior of Ti-24%V, as-quenched.

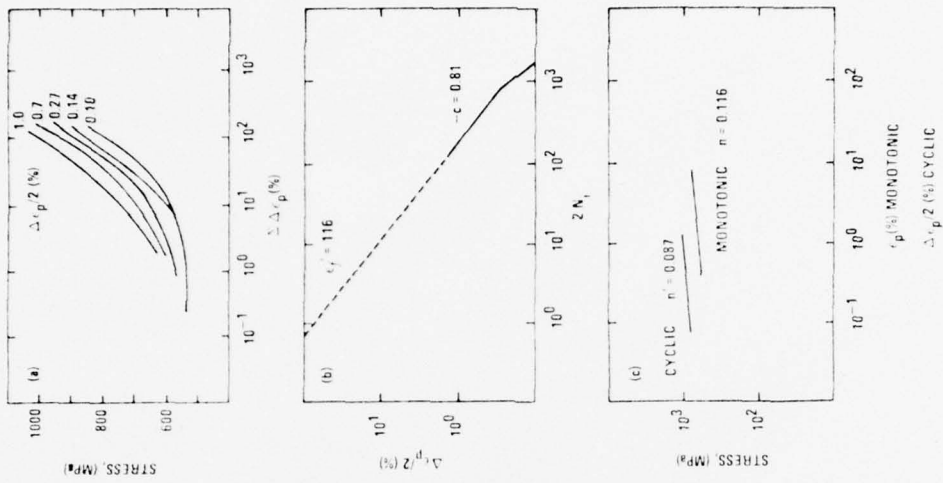


Figure 7. Low cycle fatigue behavior of Ti-24%V, aged 90 minutes at 515°C.

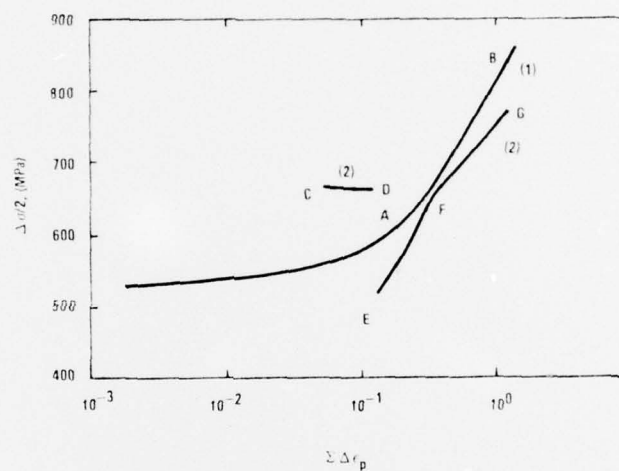
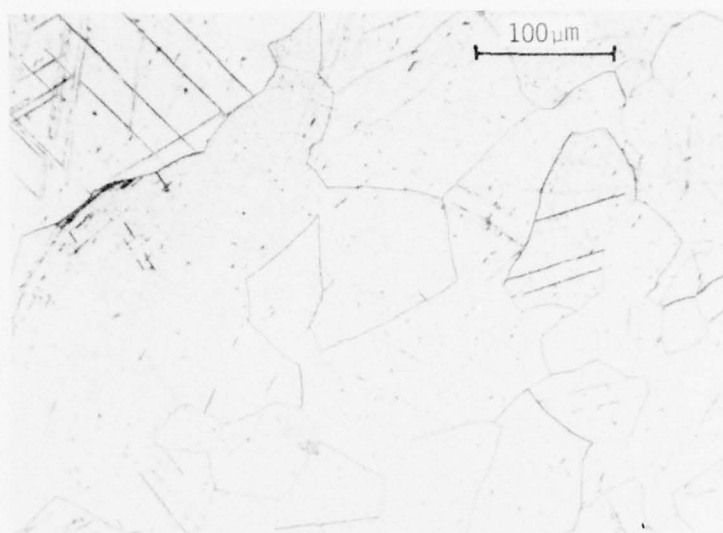
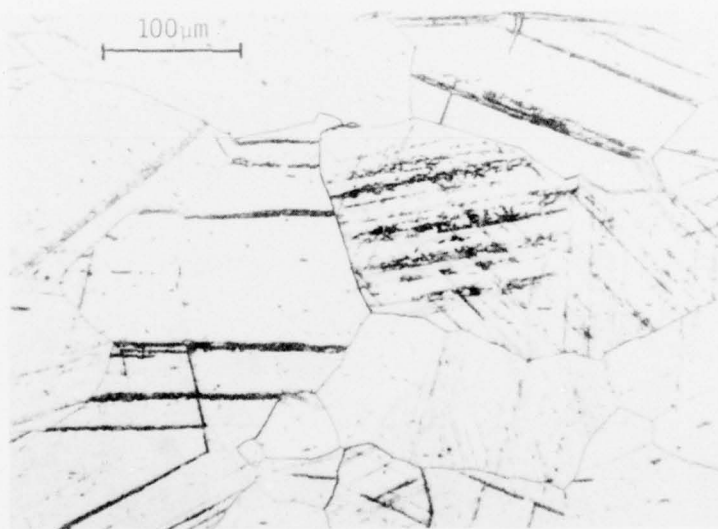


Figure 8. Cyclic hardening curves for Ti-24%V alloy using a constant strain amplitude curve 1; and a variable strain amplitude, curve 2.



a

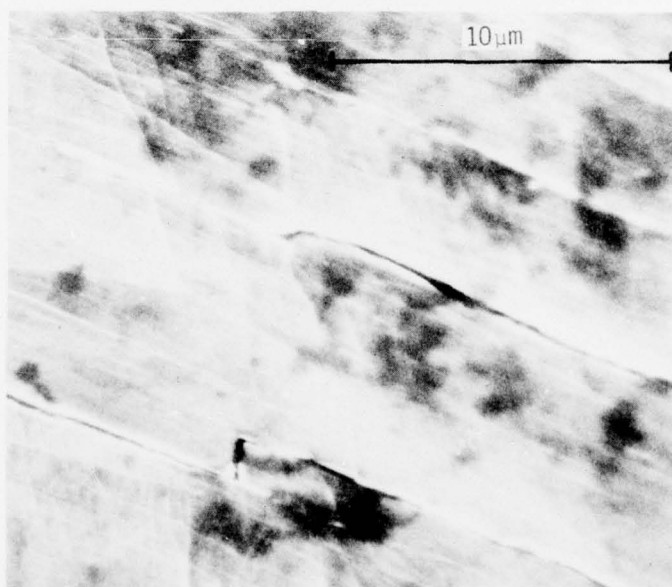


b

Figure 9. Deformation twins produced under cyclic straining of Ti-24%V. (a) constant strain amplitude, (b) variable strain amplitude.



a



b

Figure 10. Scanning electron micrograph of the surface of Ti-24%V fatigue samples. (a) concentrated slip near twin bands, (b) crack along twin bands.

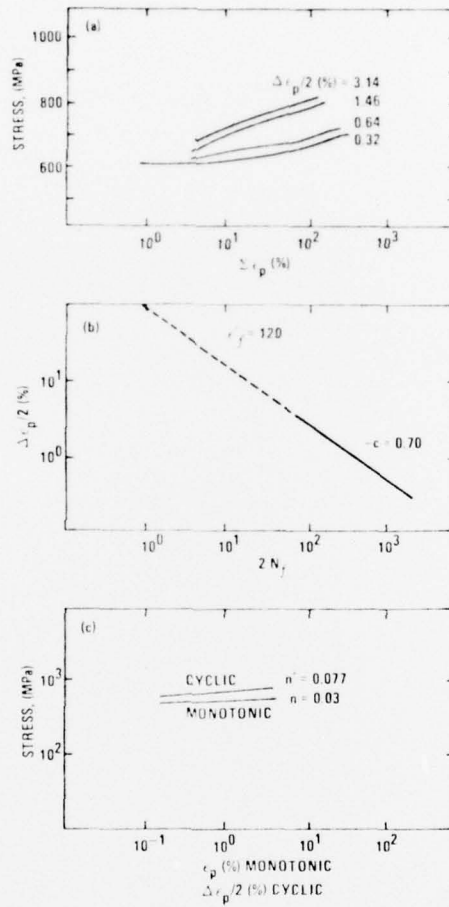


Figure 11. Low cycle fatigue behavior of Ti-28%V, as quenched.

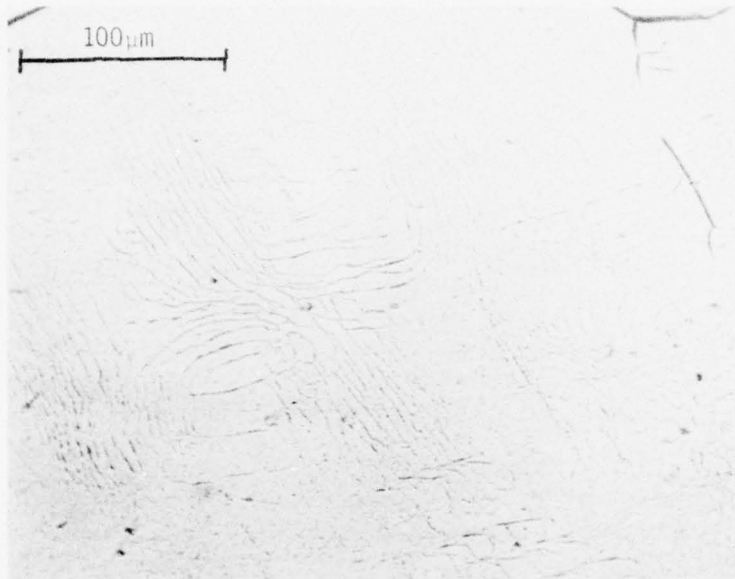
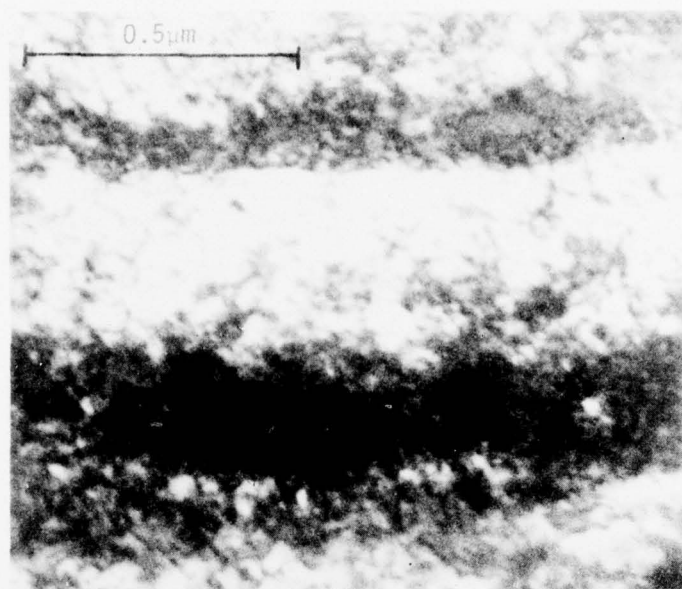
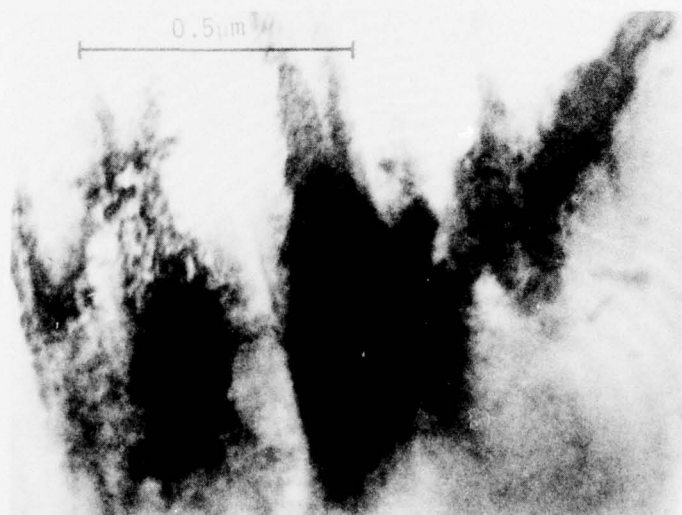


Figure 12. Optical micrograph of polished and etched cross section of Ti-28%V fatigue sample.



a



b

Figure 13. Transmission electron micrographs of Ti-28%V fatigue sample. (a) deformation bands, (b) microtwins.

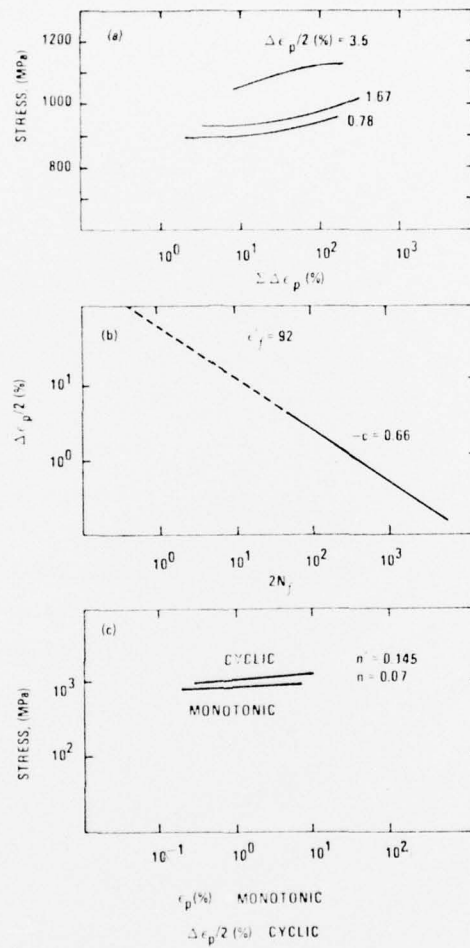
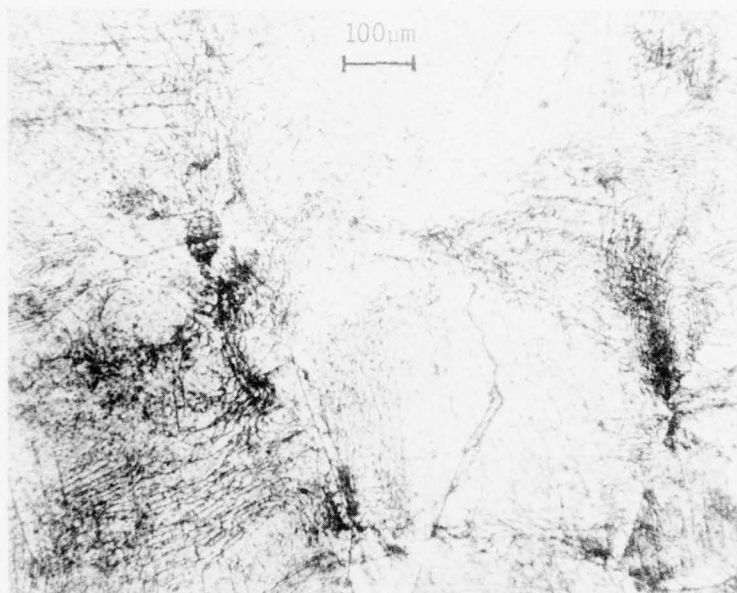
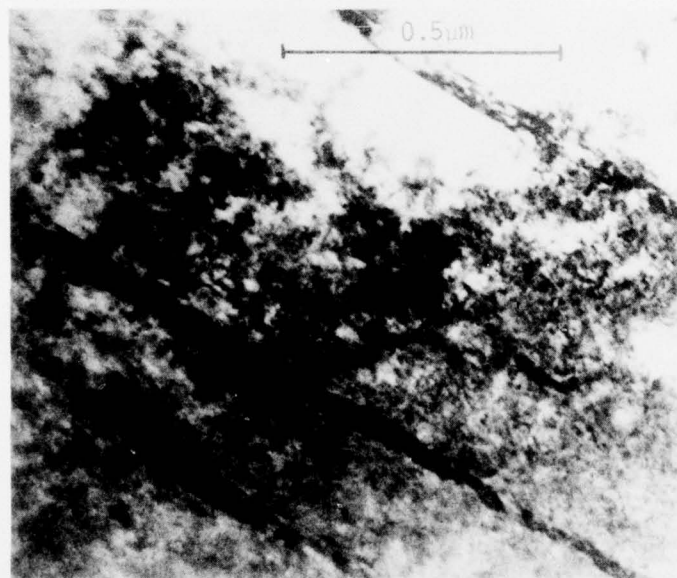


Figure 14. Low cycle fatigue behavior of Ti-28%V aged 360 minutes at 300°C.



a



b

Figure 15. Deformation structure of fatigue samples of aged 360 minutes at 300°C. (a) Optical micrograph (b) transmission electron micrograph.

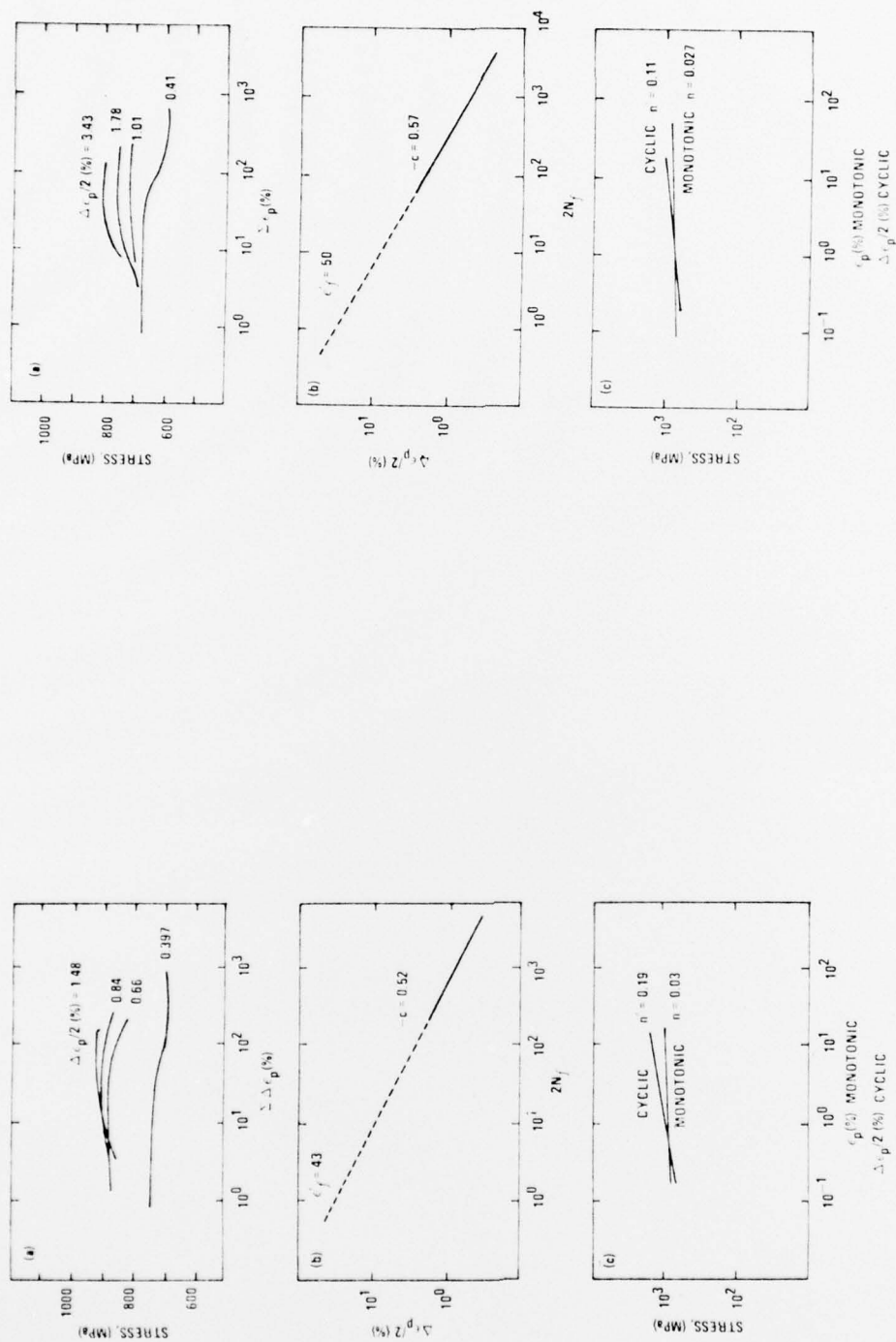


Figure 16. Low cycle fatigue behavior of Ti-32%V, as quenched.

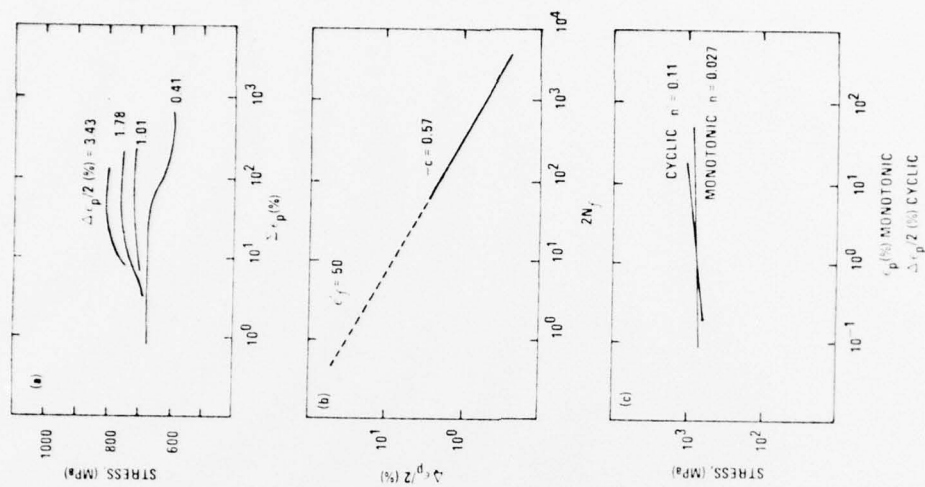


Figure 17. Low cycle fatigue behavior of Ti-36%, as quenched.

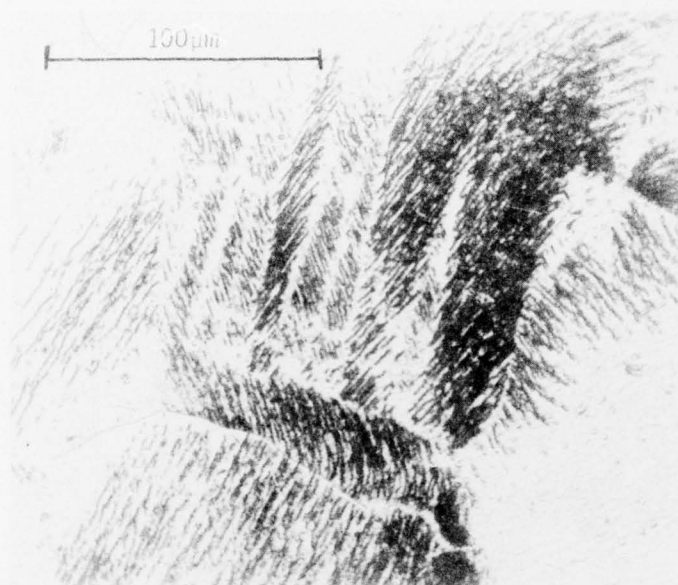
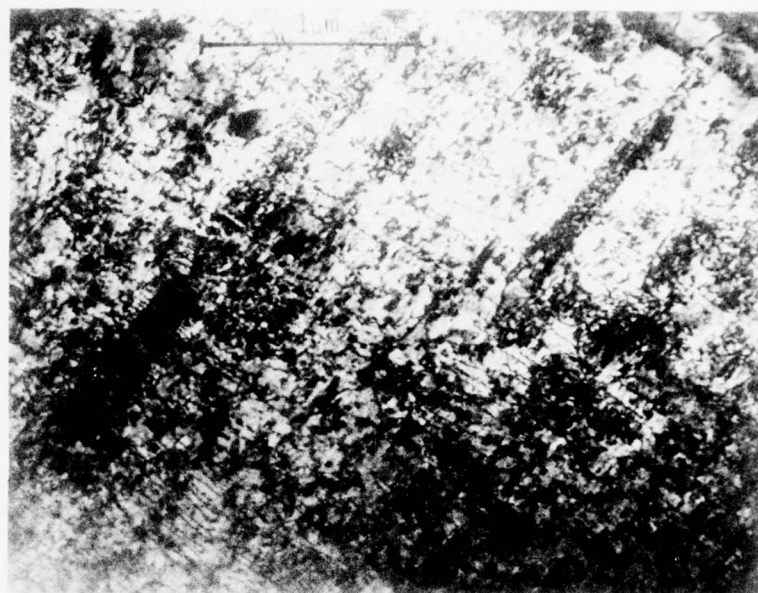
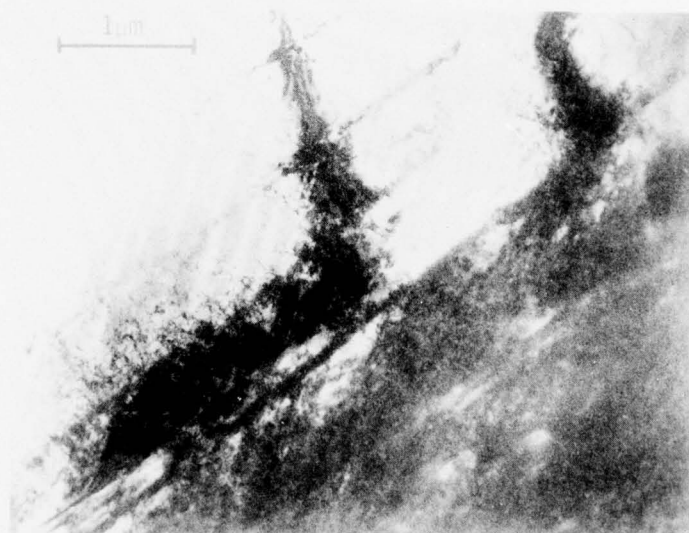


Figure 18. Optical micrograph showing typical slip markings observed in polished and etched cross sections of as quenched fatigue samples of both 32% and 36% alloys.



a



b

Figure 19. Typical deformation structure of as quenched fatigued 32% and 36%V alloys. (a) low strain amplitude where cyclic softening occurred. (b) high strain amplitude where moderate hardening occurred.

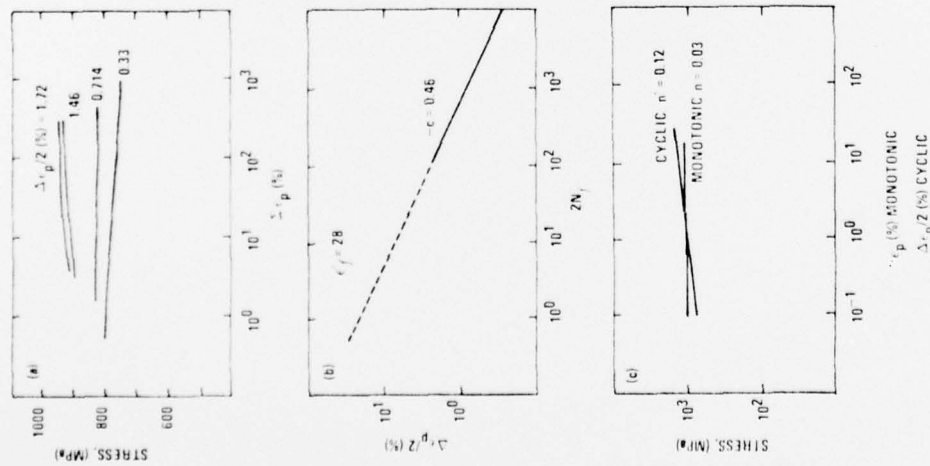


Figure 20. Low cycle fatigue behavior of Ti-32%V aged 4,700 minutes at 350°C.

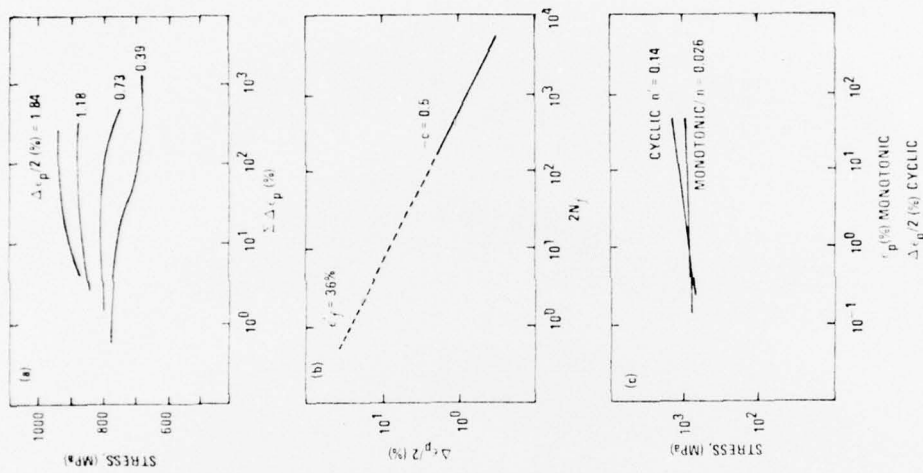


Figure 21. Low cycle fatigue behavior of Ti-36%V aged 100 minutes at 400°C.

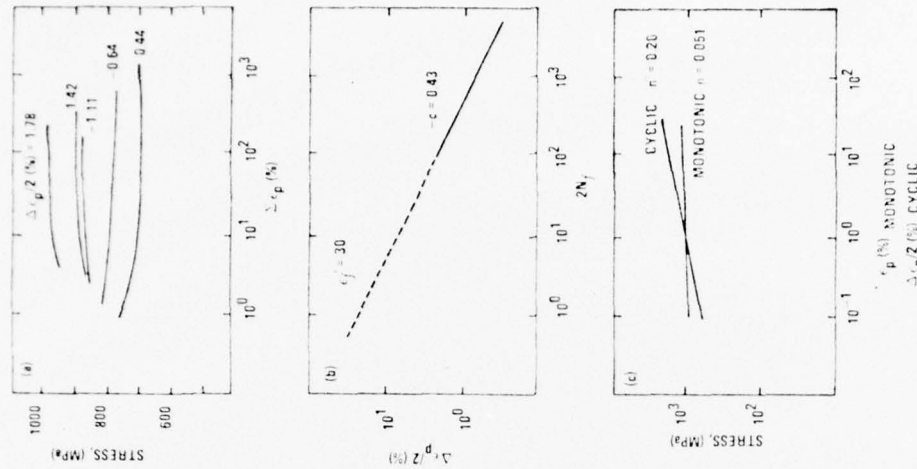


Figure 22. Low cycle fatigue behavior of Ti-36%V aged 10,000 minutes at 400°C.

SECURITY CLASSIFICATION OF THIS PAGE (When Data Entered)

REPORT DOCUMENTATION PAGE		READ INSTRUCTIONS BEFORE COMPLETING FORM
1. REPORT NUMBER 77-1	2. GOVT ACCESSION NO.	3. RECIPIENT'S CATALOG NUMBER
4. TITLE (and Subtitle) The Cyclic Stress-Strain Response of Titanium-Vanadium Alloys		5. TYPE OF REPORT & PERIOD COVERED Technical Report
7. AUTHOR(s) S. B. Chakraborty, T. K. Mukhopadhyay and E. A. Starke, Jr.		6. PERFORMING ORG. REPORT NUMBER
9. PERFORMING ORGANIZATION NAME AND ADDRESS Metallurgy Program, School of Chemical Engr. Georgia Institute of Technology, Atlanta, GA 30032		8. CONTRACT OR GRANT NUMBER(s) N00014-75-C-0349 NR 031-750
11. CONTROLLING OFFICE NAME AND ADDRESS Metallurgy Program, Office of Naval Research 800 North Quincy Street Arlington, Virginia 22217		10. PROGRAM ELEMENT, PROJECT, TASK AREA & WORK UNIT NUMBERS
14. MONITORING AGENCY NAME & ADDRESS (if different from Controlling Office)		12. REPORT DATE August 30, 1977
		13. NUMBER OF PAGES
		15. SECURITY CLASS. (of this report) unclassified
		15a. DECLASSIFICATION/DOWNGRADING SCHEDULE
16. DISTRIBUTION STATEMENT (of this Report) unlimited		
<div style="border: 1px solid black; padding: 5px; text-align: center;"> DISTRIBUTION STATEMENT A Approved for public release; Distribution Unlimited </div>		
17. DISTRIBUTION STATEMENT (of the abstract entered in Block 20, if different from Report)		
18. SUPPLEMENTARY NOTES		
19. KEY WORDS (Continue on reverse side if necessary and identify by block number) titanium alloys deformation microstructure fatigue		
20. ABSTRACT (Continue on reverse side if necessary and identify by block number) The cyclic stress-strain response of four Ti-V alloys (24, 28, 32 and 36 wt % V) which have deformation modes ranging from coarse twinning to wavy and planar slip, has been measured and correlated with deformation mode and microstructure. When coarse twinning is the primary deformation mode an anomalous Bauschinger effect, associated with untwinning during load reversal, is observed. A saturation flow stress is not obtained for the wavy slip alloy due to the intervention of microtwinning which inhibits cross slip and cell formation.		

SECURITY CLASSIFICATION OF THIS PAGE(When Data Entered)

Cyclic hardening of all alloys appears to be related, in some degree, to deformation twinning. Cyclic softening occurs for the planar slip alloys in the absence of microtwinning due to increasing mobile dislocation density.

SECURITY CLASSIFICATION OF THIS PAGE(When Data Entered)